CHEMISTRY OF MATERIALS
Cite This: Chem. Mater. 2018, 30, 6831−6838
Article
pubs.acs.org/cm

Small-Sized and Robust Chimaeric Lipopepsomes: A Simple and Functional Platform with High Protein Loading for Targeted Intracellular Delivery of Protein Toxin in Vivo

Min Qiu, Zhenqi Zhang, Yaohua Wei, Huanli Sun, Fenghua Meng, Chao Deng,* and Zhiyuan Zhong*

Biomedical Polymers Laboratory, College of Chemistry, Chemical Engineering and Materials Science, Soochow University, Suzhou, 215123, China

Supporting Information

ABSTRACT: How to chaperone protein drugs into target tumor cells in vivo is a big challenge. Here, we report on small-sized and robust chimaeric vesicles (lipopepsomes) constructed with asymmetric poly(ethylene glycol)-*b*-poly(α-aminopalmitic acid)-*b*-poly(L-aspartic acid) triblock copolypeptide as a simple and functional platform for high loading and targeted intracellular delivery of saporin, a protein toxin, in vivo. Cyclic RGD peptide-decorated chimaeric lipopepsomes (cRGD-CLP) following loading 2.0−9.4 wt % of model protein FITC-labeled cytochrome C showed a small hydrodynamic size of 81−86 nm, enhanced internalization by $\alpha_v\beta_3$-overexpressing A549 lung tumor cells, as well as remarkable accumulation of 7.73% ID/g in the cancerous lung in mice. Saporin-loaded cRGD-CLP displayed a low half-maximal inhibitory concentration of 16.3 nM to A549 cancer cells. Intriguingly, saporin-loaded cRGD-CLP at 16.7 nmol saporin equiv/kg showed a high potency in treating orthotopically xenografted A549 lung tumors, suppressed tumor progression, and remarkably improved survival rate. These chimaeric lipopepsomes provide a versatile and potential means for targeted protein therapy of various malignancies.

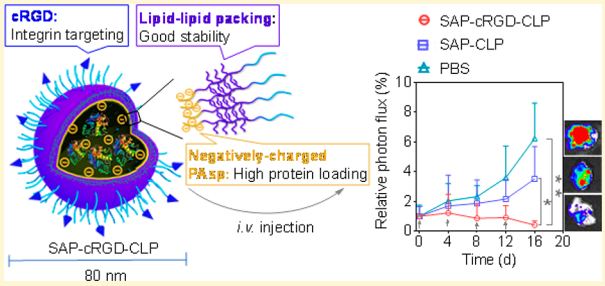

1. INTRODUCTION

Protein therapeutics with a great specificity and bioactivity has revolutionized cancer treatment.[1−5] In contrast to most clinically used proteins like Herceptin, TRAIL, interlukin-2, and interferon-γ that target biomarkers on the surface of cancer cells, therapeutic proteins with intracellular targets (e.g., saporin, granzyme B (GrB), and apoptin) are much more challenging for clinical translation because they need to overcome not only extracellular barriers but also cell membrane and intracellular barriers.[6,7] How to chaperone protein drugs into target tumor cells in vivo remains a big challenge. Different nanosystems such as liposomes,[8,9] nanoparticles,[10−15] polymeric micelles,[16−18] and nanogels[19−22] were recently explored for intracellular protein delivery, among which polymersomes with a watery lumen to load proteins and thick membrane to protect proteins from degradation appear to be a most ideal system.[23−26] One general issue with polymersomes is their low protein loading efficacy. We found that drug loading levels could be greatly enhanced by denovo-designed chimaeric polymersomes that contain short branched polyethylenimine[27,28] or poly(2-(diethyl amino)ethyl methacrylate) (PDEA)[29] in the lumen. These chimaeric polymersomes, however, expose several issues including potential toxicity concerns related to nondegradable cationic polymers and relatively complex and ill-controlled synthesis, which refrain them from clinical applications.

Here, we report facile fabrication of novel, small-sized, and robust chimaeric polymersomes from asymmetric poly(ethylene glycol)-*b*-poly(α-aminopalmitic acid)-*b*-poly(L-aspartic acid) (PEG-*b*-PAPA-*b*-PAsp) triblock copolymer as a simple and functional platform for high loading and targeted intracellular delivery of saporin, a protein toxin, in vivo (Scheme 1). Polypeptides with excellent biocompatibility, enzymatic degradability, and easy synthesis are one of the preferred materials for drug delivery.[30−35] Several polypeptide-based chemotherapeutic nanomedicines are under phases I−III clinical trials.[36,37] We recently found that PEG-*b*-PAPA diblock copolymers formed robust micelles or polymersomes, depending on hydrophilic/hydrophobic ratios, due to the existence of lipid−lipid packing.[38,39] In this contribution, we further designed chimaeric lipopepsomes from PEG-*b*-PAPA-*b*-PAsp, in which PAsp was shorter than PEG and would preferentially locate in the aqueous lumen to achieve active loading of proteins via electrostatic interactions. Our results revealed that chimaeric lipopepsomes decorated with cyclic RGD peptide

Received: July 7, 2018
Revised: September 8, 2018
Published: September 18, 2018

DOI: 10.1021/acs.chemmater.8b02868
Chem. Mater. 2018, 30, 6831−6838

Scheme 1. Schematic Illustration on Preparation of Small-Sized and Robust Chimaeric Lipopepsomes (cRGD-CLP) from PEG-*b*-PAPA-*b*-PAsp and cRGD-PEG-*b*-PAPA Copolymers for Targeted Intracellular Delivery of Saporin to Cancer Cells[a]

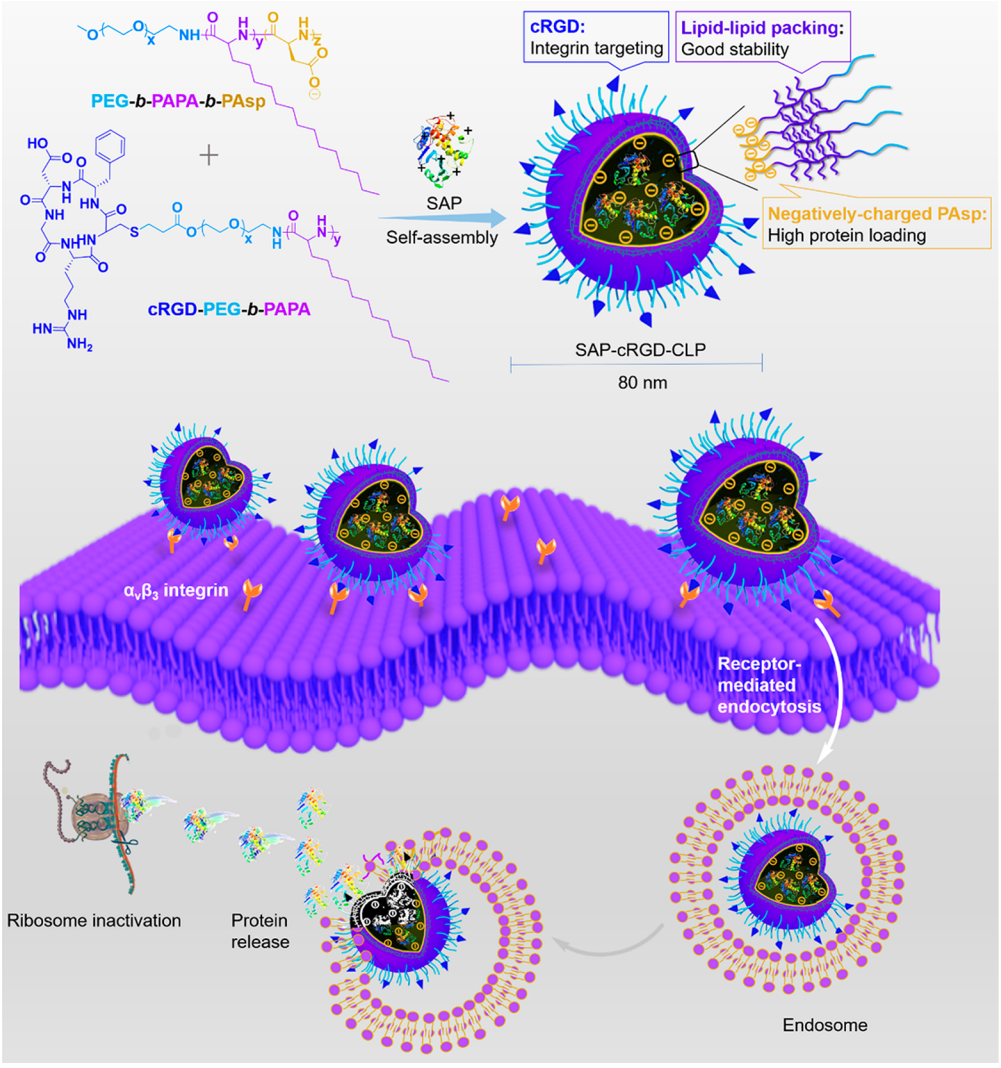

[a]cRGD-CLP was internalized in $\alpha_v\beta_3$ integrin-positive A549 lung cancer cells via a receptor-mediated mechanism, followed by endosomal membrane destabilization and cargo release.

that is known to specifically bind to $\alpha_v\beta_3$ integrin could efficiently load and deliver saporin, a protein toxin used in clinical trials for treating leukemia and lymphoma, to $\alpha_v\beta_3$ integrin-positive A549 lung tumor cells, leading to effective suppression of orthotopically xenografted A549 lung tumor in mice. These chimaeric lipopepsomes are versatile and highly promising for targeted cancer protein therapy.

2. RESULTS AND DISCUSSION

2.1. Synthesis of Poly(ethylene glycol)-*b*-poly(*α*-aminopalmitic acid)-*b*-poly(L-aspartic acid) (PEG-*b*-PAPA-*b*-PAsp) Triblock Copolypeptide. PEG-*b*-PAPA-*b*-PAsp triblock copolypeptides were synthesized through sequential polymerization of *α*-aminopalmitic acid *N*-carboxyanhydride (APA-NCA) and *β*-benzyl-L-aspartate *N*-carboxyanhydride (BLA-NCA) monomers using PEG-NH_2 as a macroinitiator, followed by removal of benzyl protection groups (Scheme 2). The structure of PEG-*b*-PAPA-*b*-PBLA was corroborated by ^{1}H NMR measurement (Figure 1A), in which characteristic signals of PEG (3.73 and 3.47 ppm), PAPA (1.80, 1.24, and 0.86 ppm), and PBLA (7.19, 5.02, and 2.92 ppm) were clear observed. The degree of polymerization (DP) of PAPA and PBLA could be calculated by comparing the integration of peaks at 0.86 (methyl protons of PAPA) and 5.02 ppm (methylene protons of PBLA) to 3.73 ppm (methylene protons of PEG). The results revealed that the DPs of PAPA and PBLA were 40 and 13, respectively, and their number-average molecular weights (M_n) were comparable to the design. Moreover, GPC measurement further confirmed that PEG-*b*-PAPA-*b*-PBLA copolypeptides had tailored M_n (24.7 kg/mol) and decent distribution (M_w/M_n = 1.31) (Table S1, Figure S1). PEG-*b*-PAPA-*b*-PAsp was obtained by acid deprotection of PEG-*b*-PAPA-*b*-PBLA in CF_3COOH using HBr/HOAc. As shown in Figure 1 B, peaks at 7.19 and 5.02 ppm attributable to the benzyl group completely disappeared, signifying the efficacious deprotection. Importantly, PAPA and PAsp blocks in PEG-*b*-PAPA-*b*-PAsp had DPs close to PAPA and PBLA blocks, respectively, in the parent PEG-*b*-PAPA-*b*-PBLA, corroborating successful synthesis of PEG-*b*-PAPA-*b*-PAsp.

DOI: 10.1021/acs.chemmater.8b02868
Chem. Mater. 2018, 30, 6831−6838

Scheme 2. Synthesis of PEG-*b*-PAPA-*b*-PAsp Triblock Copolypeptide[a]

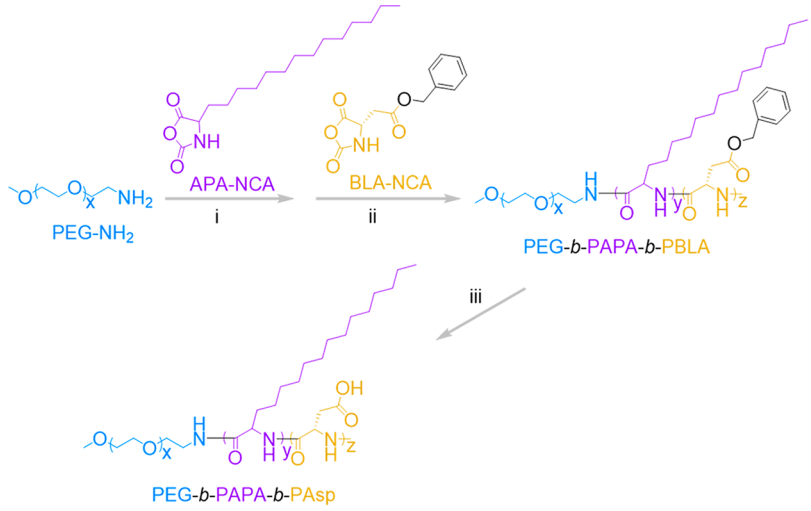

[a]Conditions: (i and ii) DMF, 35 °C, 3 d; (iii) HBr/HOAc, CF_3COOH, 0 °C, 2 h.

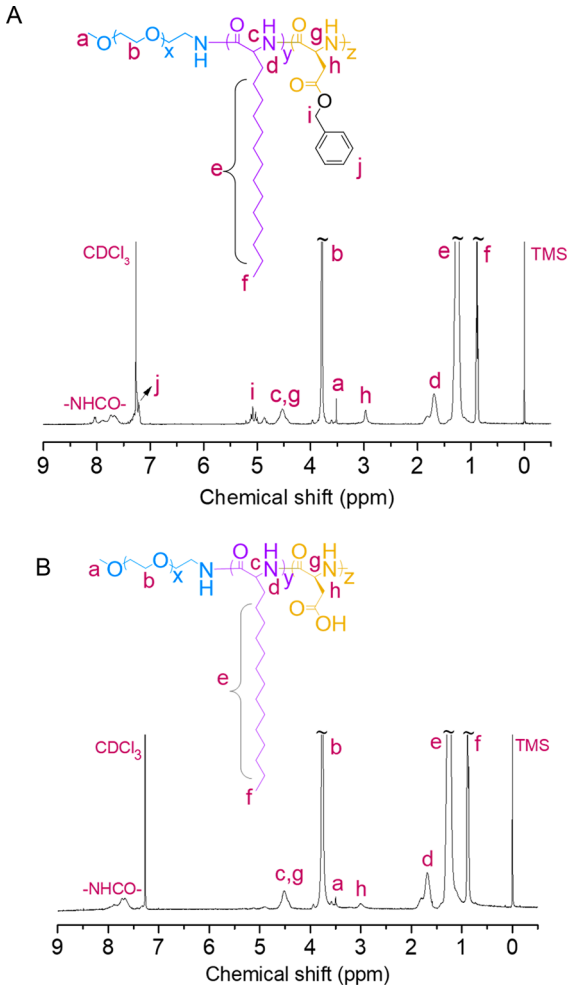

Figure 1. ^{1}H NMR spectra (600 MHz) of PEG-*b*-PAPA-*b*-PBLA (A) and PEG-*b*-PAPA-*b*-PAsp (B) in $CDCl_3/CF_3COOH$ (5/1, v/v).

2.2. Fabrication and Protein Loading of Chimaeric Lipopepsomes. The chimaeric lipopepsomes (CLP) were readily prepared through self-assembly of asymmetric PEG-*b*-PAPA-*b*-PAsp (M_n = 5.0−10.1−1.4 kg/mol) triblock copolypeptide. cRGD-targeted CLP (cRGD-CLP) could be fabricated by adding cRGD-PEG-*b*-PAPA (M_n = 6.0−11.3 kg/mol) in the process of self-assembly. The longer PEG chain in cRGD-PEG-*b*-PAPA would render cRGD peptide preferentially located toward the outer surface of lipopepsomes. Previous studies demonstrated that lipopepsomes and nanoparticles containing 20 mol % cRGD present a most pronounced targetability toward $\alpha_v\beta_3$ integrin-positive cancer cells.[39−41] cRGD-CLP exhibited small sizes of 77 nm with a narrow distribution (Figure 2A). As visualized by transmission electron microscopy (TEM), cRGD-CLP possessed a spherical morphology and vesicular structure (Figure 2B). Static light scattering (SLS) measurement revealed that cRGD-CLP had a radius of gyration (R_g) of 36.9 nm (Figure S2). An R_g/R_h ratio of 0.96 further confirms a vesicular structure of cRGD-CLP. The results from different groups have showed that asymmetric ABC triblock copolymers tended to self-assemble into chimaeric vesicles.[42−45] Interestingly, cRGD-CLP revealed a slightly negative surface charge of −9.46 mV and high colloidal stability with a critical aggregation concentration (CAC) of 2.46 mg/L (Table S2). Figure S3 displays that cRGD-CLP exhibited little size change during incubation with 10% FBS in 8 h. The high stability of cRGD-CLP could be ascribed to the tight lipid−lipid packing of PAPA segments in their membrane as demonstrated in PAPA-based micelles and symmetric polymersomes,[38,39] as well as lipid-based nanocarriers.[46,47] CLP without cRGD decoration displayed a comparable size (83 nm) and polydispersity (PDI = 0.17) to cRGD-CLP.

FITC-labeled cytochrome C (FITC-CC) was employed as a model protein to examine the protein encapsulation content (PEC) and efficiency (PEE) of cRGD-CLP. CC was used as a model because it has a similar isoelectric point (p*I*) to saporin. As shown in Table 1, FITC-CC could be efficiently encapsulated into cRGD-CLP, in which nearly quantitative loading was observed when the theoretical loading contents were 2−5 wt %. The remarkable loading level of cRGD-CLP was mainly attributed to the ionic interactions between FITC-CC and PAsp segments in the watery core. We and others have revealed that chimaeric polymersomes with charged hydrophilic block in watery core afford a markedly enhanced loading of hydrophilic drugs and proteins.[27,44] Following the

DOI: 10.1021/acs.chemmater.8b02868
Chem. Mater. 2018, 30, 6831−6838

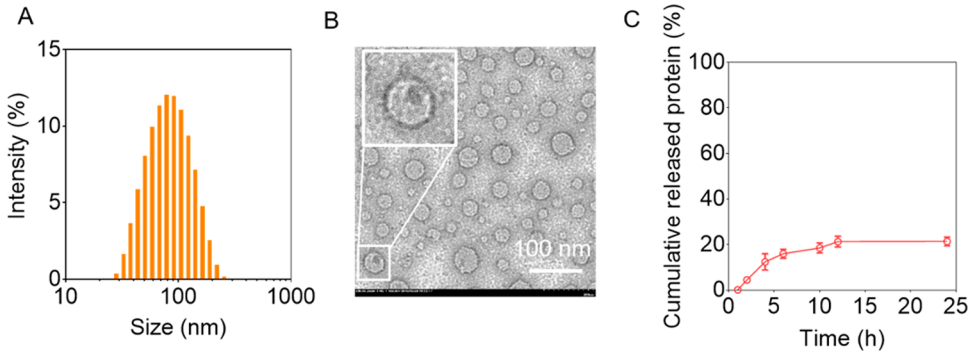

Figure 2. Characterization of cRGD-CLP. (A) Size distribution measured by DLS. (B) TEM image. (C) In vitro drug release profile of FITC-CC-cRGD-CLP in PB (n = 3).

Table 1. Characterization of FITC-CC-cRGD-CLP

	PEC (wt %)					
entry	theory	determined[a]	PEE (%)	size[b] (nm)	PDI[b]	zeta[c] (mV)
1	2.0	2.0	~100	81 ± 0.3	0.16	−6.3
2	5.0	4.9	97.8	85 ± 0.7	0.18	−5.3
3	10.0	9.4	93.6	86 ± 0.9	0.20	−6.6

[a]Determined by UV−vis spectrometry. [b]Size and PDI of FITC-CC-cRGD-CLP were determined by DLS. [c]Measured by electrophoresis.

encapsulation of FITC-CC, FITC-CC-cRGD-CLP displayed a near-neutral surface charge of around −6 mV, which was slightly higher than that of blank cRGD-CLP. cRGD-CLP loaded with 2 wt % saporin showed a small size of 66 nm (Figure S4A) and good stability in 10% FBS (Figure S4B). Zeta potential measurement indicated a surface charge of −7.7 mV. Notably, less than 25% protein was released from FITC-CC-cRGD-CLP at pH 7.4 and 37 °C in 24 h (Figure 2C), indicating that protein could be efficiently protected in the lipopepsomes during circulation. The observed protein release could be due to the fact that partial proteins are encapsulated in the membrane and released by diffusion.

2.3. Cellular Uptake and Cytotoxicity of SAP-cRGD-CLP. A549 human lung cancer cells overexpressing $\alpha_v\beta_3$ integrin were employed to evaluate the cellular uptake of FITC-CC-cRGD-CLP. CLSM measurement displayed that A549 cells treated with FITC-CC-cRGD-CLP exhibited strong FITC fluorescence in cytoplasm, whereas far weaker fluorescence was spotted in cells incubated with FITC-CC-CLP (Figure 3A). Meanwhile, flow cytometry studies revealed that FITC-CC-cRGD-CLP afforded an about 2-fold stronger FITC level in A549 cells than FITC-CC-CLP (Figure 3B). In

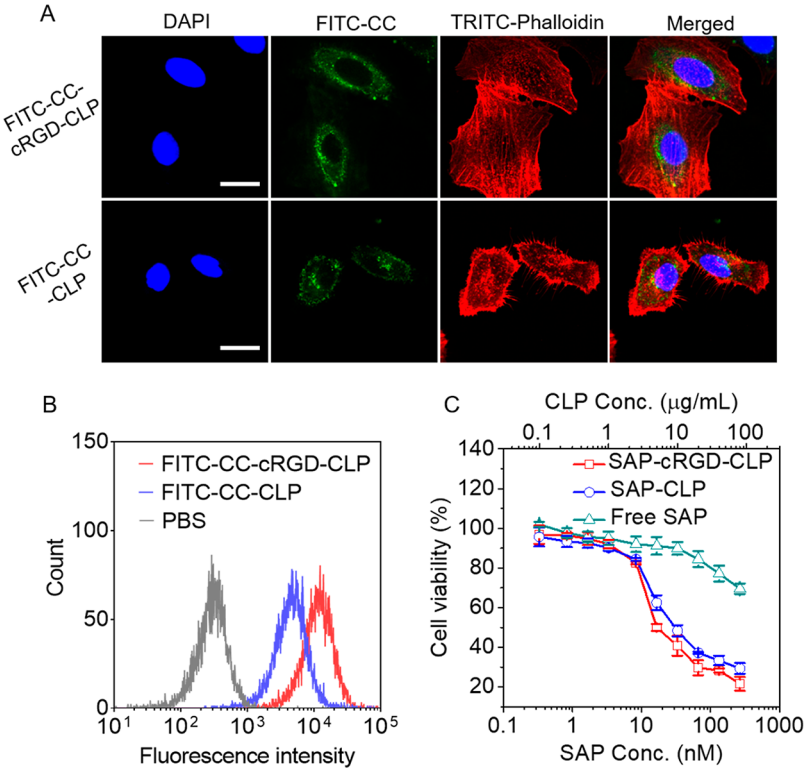

Figure 3. CLSM images (A) and flow cytometry assay (B) of A549 cells treated with FITC-CC-cRGD-CLP and FITC-CC-CLP (FITC-CC concentration 40 μg/mL) for 4 h. (C) Antiproliferative activity of SAP-cRGD-CLP toward A549 cells. Cells were incubated in SAP-cRGD-CLP solution for 4 h and in a fresh culture medium for another 44 h. Up x axis shows corresponding CLP concentrations.

DOI: 10.1021/acs.chemmater.8b02868
Chem. Mater. 2018, 30, 6831−6838

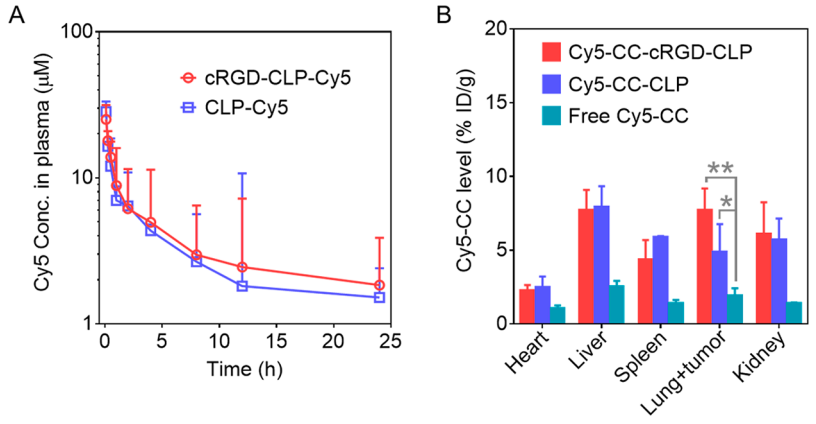

Figure 4. (A) In vivo pharmacokinetics of cRGD-CLP-Cy5 and CLP-Cy5 in normal Balb/c mice. (B) Quantified accumulation of Cy5-CC in tumor and healthy organs (n = 3, *p < 0.05, **p < 0.01).

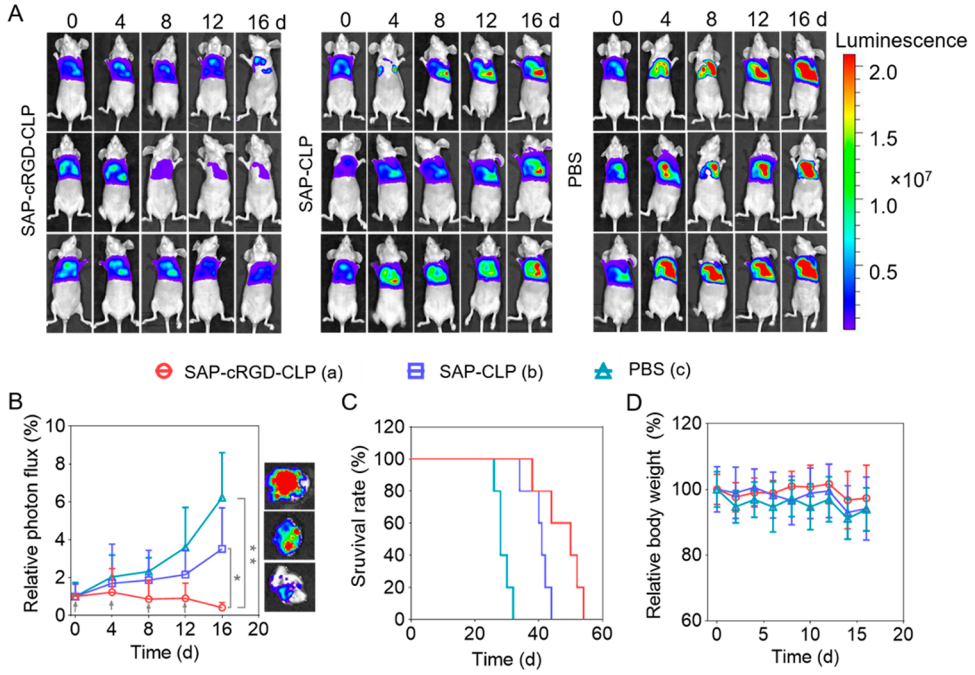

Figure 5. In vivo therapeutic effect of SAP-cRGD-CLP toward orthotopically xenografted A549-Luc human lung tumors in mice. Mice were treated on day 0, 4, 8, and 12,with a dosage of 16.7 nmol SAP equiv/kg via tail vein injection of 160 μL. (A) Bioluminescence images of mice treated with different formulations. (B) Average luminescence levels of A549-Luc xenografts in mice following different treatments. Insets are ex vivo luminescence images of lung obtained on day 16 (n = 5, *p < 0.05, **p < 0.01). (C) Survival rate of mice. Statistical analysis: SAP-cRGD-CLP vs PBS, p = 0.0018; SAP-cRGD-CLP vs SAP-CLP, p = 0.0471; SAP-CLP vs PBS, p = 0.0018 (log-rank test). (D) Body weight changes of mice treated with different formulations within 16 days.

contrast, no difference in cellular uptake was discerned for FITC-CC-cRGD-CLP and FITC-CC-CLP in $\alpha_v\beta_3$-negative MCF-7 cells (Figure S5). Notably, saporin-encapsulated cRGD-CLP (SAP-cRGD-CLP) exhibited a potent antitumor effect toward A549 cells with an IC_{50} of 16.3 nM (Figure 3C). The nontargeted control (SAP-CLP), though also inhibited cell proliferation, exhibited an obviously higher IC_{50} of 29.2 nM. As expected, cells treated with free saporin showed only a slight decrease of cell viability due to poor cellular uptake of free proteins, as also observed for free CC and GrB.[48,49] Thus, cRGD-CLP is a potent nanoplatform for intracellular delivery of therapeutic proteins to $\alpha_v\beta_3$ integrin-positive cancer cells. Of note, A549 cells treated with blank CLP and cRGD-CLP displayed nearly 100% cell viability at concentrations of 0.1−1.0 mg/mL (Figure S6). The maximum concentration of lipopepsomes employed in MTT assays was 0.08 mg/mL (Figure 3C), signifying noncytotoxicity of carrier materials.

2.4. In Vivo Pharmacokinetics, Biodistribution, and Therapeutic Efficacy of Protein-Loaded Lipopepsomes.

As shown in Figure 4A, Cy5-labeled lipopepsomes following intravenous injection into mice via a tail vein demonstrated a good circulation time, wherein cRGD-CLP-Cy5 and CLP-Cy5 exhibited a half-life ($t_{1/2,\beta}$) of 3.5 and 3.2 h, respectively. The long circulation of cRGD-CLP would facilitate systemic delivery of proteins and promote accumulation of proteins in the tumor tissue. Indeed, both Cy5-CC-cRGD-CLP and Cy5-CC-CLP groups demonstrated high protein accumulation in orthotopic A549 lung tumor xenografts following intravenous administration (Figure 4B). The Cy5-CC-cRGD-CLP group displayed an obviously higher tumor accumulation of Cy5-CC

DOI: 10.1021/acs.chemmater.8b02868
Chem. Mater. 2018, 30, 6831−6838

than the Cy5-CC-CLP group (7.73% ID/g vs 4.90% ID/g), mainly owing to the enhanced tumor targetability and retention conferred by the cRGD ligand. On the contrary, free Cy5-CC group only showed a small amount of protein accumulation (1.94% ID/g) in tumor sites. Protein therapeutics has been reported to have short half-lives and poor plasma stability due to possible enzymatic degradation.[50−52] It should further be noted that free proteins would mostly stay outside cancer cells due to poor cellular uptake.

We further evaluated the in vivo antitumor activity of SAP-cRGD-CLP in A549-Luc orthotopically xenografted human lung tumors in mice. Saporin has been employed to treat acute lymphoblastic leukemia (ALL), B-cell non-Hodgkin's lymphoma (B-NHL), T-cell acute lymphoblastic leukemia (T-ALL), and anaplastic large cell lymphoma (ALCL) in the clinical trials.[53] The tumor progression was monitored by measuring the intensity of bioluminescence that derives from A549-Luc cells. Mice were administrated with SAP-cRGD-CLP and SAP-CLP at a dosage of 16.7 nmol SAP equiv/kg every 4 days. Remarkably, Figure 5A shows that SAP-cRGD-CLP effectively inhibited tumor growth. The semiquantitative analyses of bioluminescence revealed that tumor bioluminescence on day 16 was even much lower than that on day 0 (Figure 5B). The therapeutic efficacy of SAP-cRGD-CLP was further corroborated by ex vivo tumor luminescence images collected on day 16 (Figure 5B), which clearly showed that mice administrated with SAP-cRGD-CLP revealed markedly weakened tumor luminescence intensity. Figure 5C displays that the survival time of mice was remarkably extended by treating with SAP-cRGD-CLP in comparison with PBS (median survival time: 50 vs 28 days). The nontargeted control, SAP-CLP, though less potent than SAP-cRGD-CLP, could also inhibit tumor growth and extend median survival time to 41 days. Figure 5D shows that mice in all treatment groups had no significant body weight loss, suggesting that SAP-loaded lipopepsomes induce little systemic toxicity. Remarkably, histological analysis demonstrated that mice following the treatment with SAP-cRGD-CLP possessed well-ordered lung structure and alveoli (Figure S7), signifying potent therapeutic efficacy of SAP-cRGD-CLP. In comparison, the alveoli of the mice treated with SAP-CLP and PBS were occupied by neoplasm, which would greatly truncate the respiratory function and survival time. It is evident, therefore, that chimaeric lipopepsomes provide a novel, robust, and functional platform to achieve high loading and targeted intracellular delivery of protein therapeutics in vivo.

3. CONCLUSIONS

We show that cRGD-functionalized chimaeric lipopepsomes (cRGD-CLP) achieve nearly quantitative encapsulation and targeted delivery of apoptotic proteins into the cytosol of $\alpha_v\beta_3$ integrin-positive A549 lung cancer cells, inducing potent lung tumor suppression without causing obvious systemic side effects. cRGD-CLP exhibits several notable advantages: (i) PEG-*b*-PAPA-*b*-PAsp triblock copolypeptides employed for the preparation of chimaeric polymersomes can be simply prepared in a high yield and controlled manner by NCA polymerization followed by removal of benzyl groups; (ii) cRGD-CLP exhibits a small size, excellent stability, and nearly quantitative loading of therapeutic proteins through the electrostatic and hydrogen-bonding interactions with PAsp segments in the watery core; (iii) cRGD-CLP can selectively chaperone saporin to $\alpha_v\beta_3$ integrin-positive A549 lung cancer cells, resulting in a high antitumor potency (IC_{50} = 16.3 nM); (iv) cRGD-CLP can significantly prolong circulation time and boost tumor accumulation of therapeutic proteins; and (v) saporin-loaded cRGD-CLP achieves complete inhibition of tumor growth and largely improves mice survival rate at a low dose of 16.7 nmol SAP equiv/kg in orthotopically xenografted A549 human lung tumors in mice. These robust chimaeric lipopepsomes with facile synthesis, high protein loading, and adaptive targetability have emerged as a potentially viable nanoplatform for cancer protein therapy.

4. MATERIALS AND METHODS

4.1. Synthesis of PEG-*b*-PAPA-*b*-PAsp Triblock Copolypeptides. PEG-*b*-PAPA-*b*-PAsp triblock copolypeptides were synthesized through the sequential polymerization of APA-NCA and BLA-NCA monomers in DMF solution using PEG-NH_2 as a macroinitiator, followed by the removal of benzyl groups in PEG-*b*-PAPA-*b*-poly(*β*-benzyl-L-aspartate) (PEG-*b*-PAPA-*b*-PBLA) using HBr. Typically, APA-NCA (0.52 g, 1.76 mmol) was dissolved in DMF (10.0 mL) under N_2, followed by adding the PEG-NH_2 (0.20 g, 0.04 mmol) solution in DMF (2 0 mL). The mixture was stirred at 35 °C for 72 h. Then BLA-NCA (0.18 g, 0.72 mmol) solution in DMF (2.0 mL) was added, and the reaction proceeded for another 72 h at 35 °C. The polymers were then precipitated in excess cold diethyl ether and further dried under vacuum for 48 h. Yield: 83%. ^{1}H NMR (600 MHz, Figure 1A, *δ*): 7.71 (1 H, −***NH***CO−), 7.19 (5 H, −C_6H_5), 5.02 (2 H, $C_6H_5CH_2$−), 4.45 (1 H, −CO***CH***NH−), 3.73 (4 H, −OCH_2CH_2O−), 3.47 (3 H, −OCH_3), 2.96 (2 H, −COCH_2−), 1.80 (2 H, −CH(NH)$CH_2$$CH_2$−), 1.24 (24 H, −$CH_2(CH_2)_{12}CH_3$), 0.86 (3 H, −$CH_2CH_3$).

To obtain PEG-*b*-PAPA-*b*-PAsp copolypeptides, PEG-*b*-PAPA-*b*-PBLA (0.3 g, 0.015 mmol) was dissolved in CF_3COOH (3.0 mL) and then treated with HBr (33 wt % in HOAc, 0.3 mL, 1.66 mmol) for 2 h at 0 °C. The reaction solution was precipitated using excess cold diethyl ether to obtain crude product. The resulting copolypeptides were redissolved in THF, dialyzed against water using a dialysis membrane (Spectra/Pore, MWCO, 3.5 kDa) for 48 h, and lyophilized to afford a white powder product. Yield: 80%. ^{1}H NMR (600 MHz, Figure 1B, *δ*): 7.71 (1 H, −***NH***CO−), 4.54 (1 H, −CO***CH***NH−), 3.77 (4 H, −OCH_2CH_2O−), 3.50 (3 H, −OCH_3), 3.00 (2 H, −COCH_2−), 1.76 (2 H, −CH(NH)$CH_2$$CH_2$−), 1.27 (24 H, −$CH_2(CH_2)_{12}CH_3$), 0.89 (3 H, −$CH_2CH_3$). cRGD-PEG-*b*-PAPA copolypeptide was prepared by APA-NCA polymerization using acrylate-PEG-NH_2 as a macroinitiator followed by thiol−ene reaction with cRGD-SH, according to our previous report.[38]

4.2. Formation of Chimaeric Lipopepsomes. Chimaeric lipopepsomes with or without cRGD were simply fabricated using the solvent exchange method. Taking the fabrication of cRGD-CLP as an example, cRGD-PEG-*b*-PAPA and mPEG-*b*-PAPA-*b*-PAsp were dissolved in THF at a molar ratio of 1:4 to obtain a polymer solution with a concentration of 2.0 mg/mL. Then 200 *μ*L of the polymer solution was slowly added to 800 *μ*L of PB buffer under magnetic stirring. The resulting dispersion was then transferred into a dialysis bag (MWCO 7000 Da, Spectra/Pore) and extensively dialyzed against PB for 8 h. The nontargeting CLP was fabricated similarly from asymmetric mPEG-*b*-PAPA-*b*-PAsp copolymers only.

4.3. Encapsulation and in Vitro Protein Release of cRGD-CLP. Protein-encapsulated cRGD-CLP was similarly constructed as described above for the preparation of blank cRGD-CLP, except that PB buffer was replaced with protein solutions. Cytochrome C (CC), Cy5-labeled CC (Cy5-CC), FITC-labeled CC (FITC-CC), and saporin as model proteins were employed to encapsulate in the chimaeric lipopepsomes. The amount of encapsulated protein was determined by UV−vis spectrometry. Protein encapsulation content (PEC) and efficiency (PEE) were calculated according to previously reported formula.[7]

The in vitro protein release behavior of protein-encapsulated cRGD-CLP was studied via a dialysis method. Typically, 0.5 mL of FITC-CC-cRGD-CLP (0.2 mg/mL) was loaded in a dialysis bag

DOI: 10.1021/acs.chemmater.8b02868
Chem. Mater. 2018, 30, 6831−6838

(MWCO 350 kDa), and then the dialysis bag was immersed in 25 mL of 10 mM PB. The release experiment was performed in a shaker at 37 °C, and the release medium was collected at predetermined time points. The amount of released protein was quantified using UV−vis spectrometry.

4.4. In Vivo Antitumor Efficacy of SAP-cRGD-CLP. The animal experiments were handled under protocols approved the Animal Care and Use Committee of Soochow University. The orthotopic A549-Luciferase lung cancer tumor model in mice was established as previously reported.[39] The tumor-bearing mice were allocated into three groups and administered with SAP-cRGD-CLP, SAP-CLP and PBS through intravenous injection. SAP-cRGD-CLP and SAP-CLP were used at a dosage of 16.7 nmol saporin equiv/kg and given every 4 days for a total of four injections. PBS as a negative control was administered in a same scheme. The tumor sites were visualized by IVIS Lumina II imaging system (Caliper Life Sciences) following the intraperitoneal injection of D-luciferin potassium salt solution (100 mg/kg) for 10−15 min. The values of relative body weights of mice were normalized to their weights at day 0.

■ ASSOCIATED CONTENT

Supporting Information

The Supporting Information is available free of charge on the ACS Publications website at DOI: 10.1021/acs.chemmater.8b02868.

Materials; characterization; critical aggregation concentration; cellular uptake and intracellular protein release behaviors; in vitro cytotoxicity assays; in vivo blood circulation and biodistribution; histological analysis; and statistical analysis (PDF)

■ AUTHOR INFORMATION

Corresponding Authors

*E-mail: cdeng@suda.edu.cn.
*E-mail: zyzhong@suda.edu.cn.

ORCID

Fenghua Meng: 0000-0002-8608-7738
Chao Deng: 0000-0001-7697-9874
Zhiyuan Zhong: 0000-0003-4175-4741

Notes

The authors declare no competing financial interest.

■ ACKNOWLEDGMENTS

This work was supported by the National Natural Science Foundation of China (NSFC 51773145, 51473110, 51633005, and 51761135117).

■ REFERENCES

(1) Pakulska, M. M.; Miersch, S.; Shoichet, M. S. Designer Protein Delivery: From Natural to Engineered Affinity-Controlled Release Systems. *Science* **2016**, *351*, aac4750.

(2) Mitragotri, S.; Burke, P. A.; Langer, R. Overcoming the Challenges in Administering Biopharmaceuticals: Formulation and Delivery Strategies. *Nat. Rev. Drug Discovery* **2014**, *13*, 655−672.

(3) Yu, M.; Wu, J.; Shi, J.; Farokhzad, O. C. Nanotechnology for Protein Delivery: Overview and Perspectives. *J. Controlled Release* **2016**, *240*, 24−37.

(4) Mo, R.; Jiang, T.; Di, J.; Tai, W.; Gu, Z. Emerging Micro-and Nanotechnology Based Synthetic Approaches for Insulin Delivery. *Chem. Soc. Rev.* **2014**, *43*, 3595−3629.

(5) Walsh, G. Biopharmaceutical Benchmarks 2014. *Nat. Biotechnol.* **2014**, *32*, 992−1000.

(6) Li, D.; van Nostrum, C. F.; Mastrobattista, E.; Vermonden, T.; Hennink, W. E. Nanogels for Intracellular Delivery of Biotherapeutics. *J. Controlled Release* **2017**, *259*, 16−28.

(7) Chen, J.; Zou, Y.; Deng, C.; Meng, F.; Zhang, J.; Zhong, Z. Multifunctional Click Hyaluronic Acid Nanogels for Targeted Protein Delivery and Effective Cancer Treatment in Vivo. *Chem. Mater.* **2016**, *28*, 8792−8799.

(8) Vila-Caballer, M.; Codolo, G.; Munari, F.; Malfanti, A.; Fassan, M.; Rugge, M.; Balasso, A.; de Bernard, M.; Salmaso, S. A pH-Sensitive Stearoyl-PEG-Poly(Methacryloyl Sulfadimethoxine)-Decorated Liposome System for Protein Delivery: An Application for Bladder Cancer Treatment. *J. Controlled Release* **2016**, *238*, 31−42.

(9) Kube, S.; Hersch, N.; Naumovska, E.; Gensch, T.; Hendriks, J.; Franzen, A.; Landvogt, L.; Siebrasse, J.-P.; Kubitscheck, U.; Hoffmann, B.; Merkel, R.; Csiszar, A. Fusogenic Liposomes as Nanocarriers for the Delivery of Intracellular Proteins. *Langmuir* **2017**, *33*, 1051−1059.

(10) Gause, K. T.; Wheatley, A. K.; Cui, J.; Yan, Y.; Kent, S. J.; Caruso, F. Immunological Principles Guiding the Rational Design of Particles for Vaccine Delivery. *ACS Nano* **2017**, *11*, 54−68.

(11) Wang, M.; Alberti, K.; Sun, S.; Arellano, C. L.; Xu, Q. Combinatorially Designed Lipid-Like Nanoparticles for Intracellular Delivery of Cytotoxic Protein for Cancer Therapy. *Angew. Chem., Int. Ed.* **2014**, *53*, 2893−2898.

(12) Chang, H.; Lv, J.; Gao, X.; Wang, X.; Wang, H.; Chen, H.; He, X.; Li, L.; Cheng, Y. Rational Design of a Polymer with Robust Efficacy for Intracellular Protein and Peptide Delivery. *Nano Lett.* **2017**, *17*, 1678−1684.

(13) Rahimian, S.; Kleinovink, J. W.; Fransen, M. F.; Mezzanotte, L.; Gold, H.; Wisse, P.; Overkleeft, H.; Amidi, M.; Jiskoot, W.; Lowik, C. W.; Ossendorp, F.; Hennink, W. E. Near-Infrared Labeled, Ovalbumin Loaded Polymeric Nanoparticles Based on a Hydrophilic Polyester as Model Vaccine: In Vivo Tracking and Evaluation of Antigen-Specific CD8+ T Cell Immune Response. *Biomaterials* **2015**, *37*, 469−477.

(14) Zhang, P.; Steinborn, B.; Laechelt, U.; Zahler, S.; Wagner, E. Lipo-Oligomer Nanoformulations for Targeted Intracellular Protein Delivery. *Biomacromolecules* **2017**, *18*, 2509−2520.

(15) He, H.; Chen, Y.; Li, Y.; Song, Z.; Zhong, Y.; Zhu, R.; Cheng, J.; Yin, L. Effective and Selective Anti-Cancer Protein Delivery Via All-Functions-in-One Nanocarriers Coupled with Visible Light-Responsive, Reversible Protein Engineering. *Adv. Funct. Mater.* **2018**, *28*, 1706710.

(16) Suarato, G.; Lee, S.-I.; Li, W.; Rao, S.; Khan, T.; Meng, Y.; Shelly, M. Micellar Nanocomplexes for Biomagnetic Delivery of Intracellular Proteins to Dictate Axon Formation During Neuronal Development. *Biomaterials* **2017**, *112*, 176−191.

(17) Kern, H. B.; Srinivasan, S.; Convertine, A. J.; Hockenbery, D.; Press, O. W.; Stayton, P. S. Enzyme-Cleavable Polymeric Micelles for the Intracellular Delivery of Proapoptotic Peptides. *Mol. Pharmaceutics* **2017**, *14*, 1450−1459.

(18) Kim, A.; Miura, Y.; Ishii, T.; Mutaf, O. F.; Nishiyama, N.; Cabral, H.; Kataoka, K. Intracellular Delivery of Charge-Converted Monoclonal Antibodies by Combinatorial Design of Block/Homo Polyion Complex Micelles. *Biomacromolecules* **2016**, *17*, 446−453.

(19) Chung, J. E.; Tan, S.; Gao, S. J.; Yongvongsoontorn, N.; Kim, S. H.; Lee, J. H.; Choi, H. S.; Yano, H.; Zhuo, L.; Kurisawa, M.; Ying, J. Y. Self-Assembled Micellar Nanocomplexes Comprising Green Tea Catechin Derivatives and Protein Drugs for Cancer Therapy. *Nat. Nanotechnol.* **2014**, *9*, 907−912.

(20) Zhang, X.; Malhotra, S.; Molina, M.; Haag, R. Micro- and Nanogels with Labile Crosslinks - from Synthesis to Biomedical Applications. *Chem. Soc. Rev.* **2015**, *44*, 1948−1973.

(21) Chen, J.; Ouyang, J.; Chen, Q.; Deng, C.; Meng, F.; Zhang, J.; Cheng, R.; Lan, Q.; Zhong, Z. EGFR and CD44 Dual-Targeted Multifunctional Hyaluronic Acid Nanogels Boost Protein Delivery to Ovarian and Breast Cancers in Vitro and in Vivo. *ACS Appl. Mater. Interfaces* **2017**, *9*, 24140−24147.

(22) Dutta, K.; Hu, D.; Zhao, B.; Ribbe, A. E.; Zhuang, J.; Thayumanavan, S. Templated Self-Assembly of a Covalent Polymer Network for Intracellular Protein Delivery and Traceless Release. *J. Am. Chem. Soc.* **2017**, *139*, 5676−5679.

DOI: 10.1021/acs.chemmater.8b02868
Chem. Mater. 2018, 30, 6831−6838

(23) Hu, X.; Zhang, Y.; Xie, Z.; Jing, X.; Bellotti, A.; Gu, Z. Stimuli-Responsive Polymersomes for Biomedical Applications. *Biomacromolecules* **2017**, *18*, 649−673.
(24) van Dongen, S. F. M.; Verdurmen, W. P. R.; Peters, R. J. R. W.; Nolte, R. J. M.; Brock, R.; van Hest, J. C. M. Cellular Integration of an Enzyme-Loaded Polymersome Nanoreactor. *Angew. Chem., Int. Ed.* **2010**, *49*, 7213−7216.
(25) Lee, J. S.; Feijen, J. Polymersomes for Drug Delivery: Design, Formation and Characterization. *J. Controlled Release* **2012**, *161*, 473−483.
(26) Qi, W.; Zhang, Y.; Wang, J.; Tao, G.; Wu, L.; Kochovski, Z.; Gao, H.; Chen, G.; Jiang, M. Deprotection-Induced Morphology Transition and Immuno-Activation of Glyco-Vesicles: A Strategy of Smart Delivery Polymersomes. *J. Am. Chem. Soc.* **2018**, *140*, 8851−8857.
(27) Zou, Y.; Zheng, M.; Yang, W.; Meng, F.; Miyata, K.; Kim, H. J.; Kataoka, K.; Zhong, Z. Virus-Mimicking Chimaeric Polymersomes Boost Targeted Cancer Sirna Therapy in Vivo. *Adv. Mater.* **2017**, *29*, 1703285.
(28) Yang, W.; Yang, L.; Xia, Y.; Cheng, L.; Zhang, J.; Meng, F.; Yuan, J.; Zhong, Z. Lung Cancer Specific and Reduction-Responsive Chimaeric Polymersomes for Highly Efficient Loading of Pemetrexed and Targeted Suppression of Lung Tumor in Vivo. *Acta Biomater.* **2018**, *70*, 177−185.
(29) Sun, H.; Meng, F.; Cheng, R.; Deng, C.; Zhong, Z. Reduction and pH Dual-Bioresponsive Crosslinked Polymersomes for Efficient Intracellular Delivery of Proteins and Potent Induction of Cancer Cell Apoptosis. *Acta Biomater.* **2014**, *10*, 2159−2168.
(30) Song, Z.; Han, Z.; Lv, S.; Chen, C.; Chen, L.; Yin, L.; Cheng, J. Synthetic Polypeptides: From Polymer Design to Supramolecular Assembly and Biomedical Application. *Chem. Soc. Rev.* **2017**, *46*, 6570−6599.
(31) Deming, T. J. Synthesis of Side-Chain Modified Polypeptides. *Chem. Rev.* **2016**, *116*, 786−808.
(32) He, C.; Zhuang, X.; Tang, Z.; Tian, H.; Chen, X. Stimuli-Sensitive Synthetic Polypeptide-Based Materials for Drug and Gene Delivery. *Adv. Healthcare Mater.* **2012**, *1*, 48−78.
(33) Liarou, E.; Varlas, S.; Skoulas, D.; Tsimblouli, C.; Sereti, E.; Dimas, K.; Iatrou, H. Smart Polymersomes and Hydrogels from Polypeptide-Based Polymer Systems through Alpha-Amino Acid N-Carboxyanhydride Ring-Opening Polymerization. From Chemistry to Biomedical Applications. *Prog. Polym. Sci.* **2018**, *83*, 28−78.
(34) Deng, C.; Wu, J.; Cheng, R.; Meng, F.; Klok, H.-A.; Zhong, Z. Functional Polypeptide and Hybrid Materials: Precision Synthesis Via Alpha-Amino Acid N-Carboxyanhydride Polymerization and Emerging Biomedical Applications. *Prog. Polym. Sci.* **2014**, *39*, 330−364.
(35) Oliveira, H.; Perez-Andres, E.; Thevenot, J.; Sandre, O.; Berra, E.; Lecommandoux, S. Magnetic Field Triggered Drug Release from Polymersomes for Cancer Therapeutics. *J. Controlled Release* **2013**, *169*, 165−170.
(36) Cabral, H.; Kataoka, K. Progress of Drug-Loaded Polymeric Micelles into Clinical Studies. *J. Controlled Release* **2014**, *190*, 465−476.
(37) Nishiyama, N.; Matsumura, Y.; Kataoka, K. Development of Polymeric Micelles for Targeting Intractable Cancers. *Cancer Sci.* **2016**, *107*, 867−874.
(38) Qiu, M.; Ouyang, J.; Sun, H.; Meng, F.; Cheng, R.; Zhang, J.; Cheng, L.; Lan, Q.; Deng, C.; Zhong, Z. Biodegradable Micelles Based on Poly(Ethylene Glycol)-b-Polylipopeptide Copolymer: A Robust and Versatile Nanoplatform for Anticancer Drug Delivery. *ACS Appl. Mater. Interfaces* **2017**, *9*, 27587−27595.
(39) Qiu, M.; Sun, H.; Meng, F.; Cheng, R.; Zhang, J.; Deng, C.; Zhong, Z. Lipopepsomes: A Novel and Robust Family of Nano-Vesicles Capable of Highly Efficient Encapsulation and Tumor-Targeted Delivery of Doxorubicin Hydrochloride in Vivo. *J. Controlled Release* **2018**, *272*, 107−113.
(40) Makino, J.; Cabral, H.; Miura, Y.; Matsumoto, Y.; Wang, M.; Kinoh, H.; Mochida, Y.; Nishiyama, N.; Kataoka, K. cRGD-Installed Polymeric Micelles Loading Platinum Anticancer Drugs Enable Cooperative Treatment against Lymph Node Metastasis. *J. Controlled Release* **2015**, *220*, 783−791.
(41) Arosio, D.; Casagrande, C. Advancement in Integrin Facilitated Drug Delivery. *Adv. Drug Delivery Rev.* **2016**, *97*, 111−143.
(42) Konishcheva, E. V.; Zhumaev, U. E.; Meier, W. P. PEO-b-PCL-b-PMOXA Triblock Copolymers: From Synthesis to Microscale Polymersomes with Asymmetric Membrane. *Macromolecules* **2017**, *50*, 1512−1520.
(43) Blanazs, A.; Massignani, M.; Battaglia, G.; Armes, S. P.; Ryan, A. J. Tailoring Macromolecular Expression at Polymersome Surfaces. *Adv. Funct. Mater.* **2009**, *19*, 2906−2914.
(44) Li, J.; Xiao, S.; Xu, Y.; Zuo, S.; Zha, Z.; Ke, W.; He, C.; Ge, Z. Smart Asymmetric Vesicles with Triggered Availability of Inner Cell-Penetrating Shells for Specific Intracellular Drug Delivery. *ACS Appl. Mater. Interfaces* **2017**, *9*, 17727−17735.
(45) Chen, P.; Qiu, M.; Deng, C.; Meng, F.; Zhang, J.; Cheng, R.; Zhong, Z. pH-Responsive Chimaeric Pepsomes Based on Asymmetric Poly(Ethylene Glycol)-b-Poly(L-Leucine)-b-Poly(L- Glutamic Acid) Triblock Copolymer for Efficient Loading and Active Intracellular Delivery of Doxorubicin Hydrochloride. *Biomacromolecules* **2015**, *16*, 1322−1330.
(46) Zhang, L.; Chan, J. M.; Gu, F. X.; Rhee, J.-W.; Wang, A. Z.; Radovic-Moreno, A. F.; Alexis, F.; Langer, R.; Farokhzad, O. C. Self-Assembled Lipid-Polymer Hybrid Nanoparticles: A Robust Drug Delivery Platform. *ACS Nano* **2008**, *2*, 1696−1702.
(47) Wang, G.; Wang, J.; Wu, W.; To, S. S. T.; Zhao, H.; Wang, J. Advances in Lipid-Based Drug Delivery: Enhancing Efficiency for Hydrophobic Drugs. *Expert Opin. Drug Delivery* **2015**, *12*, 1475−1499.
(48) Li, S.; Zhang, J.; Deng, C.; Meng, F.; Yu, L.; Zhong, Z. Redox-Sensitive and Intrinsically Fluorescent Photoclick Hyaluronic Acid Nanogels for Traceable and Targeted Delivery of Cytochrome C to Breast Tumor in Mice. *ACS Appl. Mater. Interfaces* **2016**, *8*, 21155−21162.
(49) Yang, W.; Xia, Y.; Zou, Y.; Meng, F.; Zhang, J.; Zhong, Z. Bioresponsive Chimaeric Nanopolymersomes Enable Targeted and Efficacious Protein Therapy for Human Lung Cancers in Vivo. *Chem. Mater.* **2017**, *29*, 8757−8765.
(50) Pisal, D. S.; Kosloski, M. P.; Balu-Iyer, S. V. Delivery of Therapeutic Proteins. *J. Pharm. Sci.* **2010**, *99*, 2557−2575.
(51) Vaishya, R.; Khurana, V.; Patel, S.; Mitra, A. K. Long-Term Delivery of Protein Therapeutics. *Expert Opin. Drug Delivery* **2015**, *12*, 415−440.
(52) Wu, X.; He, C.; Wu, Y.; Chen, X.; Cheng, J. Nanogel-Incorporated Physical and Chemical Hybrid Gels for Highly Effective Chemo-Protein Combination Therapy. *Adv. Funct. Mater.* **2015**, *25*, 6744−6755.
(53) Giansanti, F.; Flavell, D. J.; Angelucci, F.; Fabbrini, M. S.; Ippoliti, R. Strategies to Improve the Clinical Utility of Saporin-Based Targeted Toxins. *Toxins* **2018**, *10*, 82.

DOI: 10.1021/acs.chemmater.8b02868
Chem. Mater. 2018, 30, 6831−6838